Chimeric fusions of subunit IV and PetL in the b_6f complex of *Chlamydomonas reinhardtii :* structural implications and consequences on State Transitions*

Francesca Zito[‡,‖], Joëlle Vinh[§], Jean-Luc Popot[‡] & Giovanni Finazzi[¶]

From [‡]UMR 7099, CNRS and Université Paris-7, Institut de Biologie Physico-Chimique, 13 rue Pierre et Marie Curie, F-75005 Paris, France, [§]UMR 7637, Ecole Supérieure de Physique et Chimie Industrielles de la Ville de Paris, 10 rue Vauquelin, F-75005 Paris, France, and [¶]Centro di Studio del C.N.R. sulla Biologia Cellulare e Molecolare delle Piante, Università degli Studi di Milano, via Celoria 26, 20133, Milano Italy, and UMR 1261, CNRS and Université Paris-7, Institut de Biologie Physico-Chimique, 13 rue Pierre et Marie Curie, F-75005 Paris, France

*This work was supported by the Centre National de la Recherche Scientifique, the Université Paris-7, the Consiglio Nazionale delle Richerche, and the CNR-CNRS "Cooperazione italo-francese" project 5295. F.Z. was the recipient of a fellowship from "La société de secours des amis des sciences", Paris, France.

‖ To whom correspondence should be addressed : UMR 7099, Institut de Biologie Physico-Chimique, 13 rue Pierre et Marie Curie, F-75005 Paris, France ; francesca.zito@ibpc.fr.

Running title: Subunit IV-PetL chimeras in cytochrome b_6f complex

Additional keywords : PetG, PetM, PetN, transmembrane topology, mass spectrometry, State Transitions, protein phosphorylation.

The cytochrome b_6f complex of *Chlamydomonas reinhardtii* contains four large subunits and at least three small ones, PetG, PetL and PetM, whose role and location are unknown. Chimeric proteins have been constructed, in which the C-terminus of subunit IV is fused to either one or the other of the two putative N-termini of PetL. Biochemical and functional analysis of the chimeras together with mass spectrometry analysis of the wild-type (WT) complex lead to the following conclusions : *i)* neither a free subunit IV C-terminus nor a free PetL N-terminus is required for assembly of the b_6f complex ; *ii)* the first AUG codon in the sequence of gene *petL* is used for initiation ; *iii)* the N-terminus of WT PetL lies in the lumen ; *iv)* in the WT complex, the N-terminus of PetL and the C-terminus of subunit IV are within reach of each other ; *v)* the purified b_6f complex from *C. reinhardtii* contains an eight, hitherto unrecognized subunit, PetN ; *vi)* the ability to perform State Transitions is lost in the chimeric mutants, even though *vii)* the Q-cycle is unaffected. A structural hypothesis is presented to account for this peculiar phenotype.

Cytochrome b_6f catalyzes electron transfer from plastoquinol to a hydrosoluble acceptor (plastocyanin or cytochrome c_6), while building up a transmembrane proton gradient. The b_6f complex is found in higher plants, in algae and in cyanobacteria (1). Purified cytochrome b_6f from the fresh-water unicellular alga *Chlamydomonas reinhardtii* is a super-dimer (2). Each "monomer" contains four large subunits : cytochromes *f* and b_6, subunit IV (suIV)[1] and the Rieske iron-sulfur protein (3). Cytochrome b_6 and suIV are respectively homologous to the N- and C-terminal moieties of cytochrome *b*, the chloroplast Rieske protein to its mitochondrial homonym. Cytochrome *f* and cytochrome c_1, despite their functional similarities, are not evolutionarily related (see ref. 1). Purified preparations of cytochrome b_6f also contain several very small subunits ($M_r \approx 4$ kDa), which have no homologues in cytochrome bc_1. Each of them is thought to span the membrane as a single α-helix. Subunits PetG and PetL have been encountered in all b_6f complexes studied thus far (4-7). Subunit PetM (formerly called PetX) has been found in *C. reinhardtii* (3,5,6,8), in higher plants (6), and in cyanobacteria (9). Subunit PetN hitherto has been observed only in *Nicotiana tabacum* (10), but a gene encoding a homologous protein is present in the nuclear DNA of *C. reinhardtii* (11). The role of the 4-kDa subunits is uncertain. Deletion of the *petG* gene in *C. reinhardtii* (12) or of the *petN* gene in Tobacco (10) prevents accumulation of the b_6f complex, while deletion of the *petM* gene in *Synechocystis* PCC 6803 does not interfere with the assembly of a functional complex (9). As discussed below, the case of PetL is intermediate.

The structure of several forms of cytochrome bc_1 has been solved by X-ray crystallography (reviewed in ref. 1). As regards the b_6f complex, X-ray data are limited to the extra-membrane, catalytic domains of cytochrome *f* and the Rieske protein (for a review, see ref. 1). Low-resolution electron microscopy projection maps of the whole complex reveal an arran

[1] Footnote 1

gement of transmembrane helices around the C2 axis of symmetry of the dimer that looks similar to that in cytochrome bc_1, making it possible to propose tentative positions in the map for most of the b_6f transmembrane helices (see ref. 13). Since cytochrome bc_1 does not contain peptides homologous to the small b_6f subunits, its structure on the other hand is of little help in trying to understand their arrangement and role in thee b_6f complex. Yet, some of the structural divergences between the two types of cytochromes, including their dissimilar subunit and prosthetic group (see ref. 14) complements, must bear on functional differences.

One of those, which is particularly relevant to the present work, is the role of cytochrome b_6f in the so-called State Transitions, a regulatory process whereby photosynthetic organisms balance the supply of excitons between the reaction centers of the two photosystems (PS) (15,16). Transition from State 1 to State 2 results from the transfer of a fraction of the outer PSII light harvesting complex (LHCII) to PSI, a process triggered by the phosphorylation of LHCII (16,17). During a State 2 → State 1 transition, LHCII is dephosphorylated and re-associates with PSII (16). Modulation of the phosphorylation state of antenna proteins result from the opposite actions of an LHCII-kinase, the activation of which is redox-dependent (18), and a phosphatase, which is generally considered to be permanently active (19). Recent data however have suggested a possible regulatory role of an immunophilin-like protein (20). Phosphorylation is activated by the reduction of the plastoquinone (PQ) pool (18,21) and requires the presence of cytochrome b_6f (22,23). The nature of the kinase is still obscure, even though its presence has been reported in partially purified preparations of higher plant cytochrome b_6f complexes (24). In *Arabidopsis thaliana*, the consequences of expressing antisense RNAs (25) suggest the involvement in State Transitions of a family of thylakoid-associated – presumably transmembrane – kinases (TAKs) (26). Although the molecular mechanism by which the redox state of the PQ pool controls the kinase is not known, it has been shown *in vitro* with thylakoid preparations from spinach (27,28) and *in vivo* in *C.*

reinhardtii cells (23) that it depends on plastoquinol (PQH_2) binding to the oxidizing (Q_o) site of the cytochrome b_6f complex.

The original aim of the present work was to gather information about the location and transmembrane topology of subunit PetL. PetL is strictly required neither for the accumulation nor for the function of cytochrome b_6f ; in its absence, however, the complex becomes unstable *in vivo* in aging cells and labile *in vitro* (7). The mRNA sequence deduced from that of the chloroplast gene *petL* features two possible AUG codons (7). The N-terminus of PetL being blocked (3), it is not known which is used for initiation. The distribution of basic residues in the predicted sequence of PetL suggests that, whatever the N-terminus is, it is likely to lie in the thylakoid lumen (7). If this prediction is correct, the C-terminus of suIV and the N-terminus of PetL lie in the same subcellular compartment. In the present study, we have fused the genes coding for suIV (*petD*) and for PetL by linking either the first or the second of the putative initiation codons for PetL to that coding for the last residue of suIV (Fig. 1), and examined the expression and accumulation of the chimeric constructs. *In vivo* functional analysis using time-resolved spectroscopy and fluorescence measurements revealed unusual properties : the chimeric mutants are unimpaired as far as the Q-cycle is concerned, but their State Transitions are blocked. In order to narrow down the range of possible structural interpretations of these observations, the length of mature PetL has been directly investigated by mass spectrometry (MS) analysis of the WT complex. The phenotype of the chimeric strains provides interesting insights into the nature of transconformations that could account for the activation of the kinase. In the course of the MS study, evidence was also obtained regarding the presence in *Chlamydomonas* b_6f of a hitherto unrecognized subunit, PetN, which was confirmed immunologically.

Fig. 1

EXPERIMENTAL PROCEDURES

Materials – Sources of chemicals not indicated in the text were as described in ref. 3.

Strains, media, and growth conditions – A WT *C. reinhardtii* strain (mt+) derived from strain 137c and a Δ*petL* deletion strain (7) were used as controls. The deletion strain Δ*petD* (mt+) (29) was used as recipient strain in chloroplast transformation experiments. WT and mutant strains were grown on Tris-acetate-phosphate (TAP) medium (pH 7.2) at 25° C under dim light (5-6 $\mu E.m^{-2}.s^{-1}$) (30). Cells were harvested during exponential growth phase and resuspended in a minimal medium (31). They were placed in State 1 and State 2 conditions in darkness, either by vigorous stirring to ensure a strong aeration (State 1, ref. 32) or by addition of 5 μM FCCP (State 2, ref. 33).

Plasmids, oligonucleotides and mutagenesis – Plasmids encoding chimeric constructs were created by PCR-mediated site-directed mutagenesis. To generate the fusion between the *petD* and *petL* genes, plasmid pdDΔHI.I (29), carrying the entire coding sequence of *petD*, was used as template in PCR reactions using oligonucleotides petDDir (CGCGCTTAAGTTA**AGATCT**AAAATTTTAAATTTCCCTCTA) and petDRev (CGCGCTTAAGAATAAACCTAAAGTTAAAGAAATATCAA) as primers and the Arrow™ Taq DNA polymerase according to the manufacturer's instructions. The PCR product was digested with *Afl*II at a restriction site (underlined in the sequence) introduced along with the *Bgl*II site (indicated in bold), and religated onto itself to yield plasmid pdDΔFus. Plasmid pR23 (34), which carries the *psaC* operon (7), was used as template in PCR reactions using oligonucleotides petLDirL (GCGCTTAAGTATGATTTTGATTTTAATTATATCCATAT) or petLDirS (GCGCTTAAGTATGTTAACAATCACAAGTTACGTAGGT), homologous respectively to the regions of the putative first or second AUG initiation codons of the *petL* gene (see *Results*), and reverse oligonucleotide petLRev

(CGC**AGATCT**CGAGTTAGATAAGTTTTACAACTTTTAAAAGACCT) as primers. PCR products were digested with *Afl*II and *Bgl*II and cloned into plasmid pdDΔFus digested with the same enzyme, yielding plasmids p*DL*L and p*DL*S. The sequence of these plasmids was checked.

Plasmids p*DL*L and p*DL*S were introduced by biolistic transformation (35) into the chloroplast genome of the deletion strain Δ*petD* (29). Phototrophic transformants were selected for growth on minimun medium according to ref. 29. The resulting mutant strains, *DL*L and *DL*S, were in turn used as recipient strains for biolistic transformation by plasmid p*ycf7*::*aadA* (a kind gift of Y. Takahashi, Okayama University), which carries an *aadA* cassette conferring resistance to spectinomycin inserted at the *Sna*BI site within the *petL* coding sequence (7). Transformed clones were selected on TAP medium containing spectinomycin (100 $\mu g.ml^{-1}$) and subcloned several times on selective medium until they reached homoplasmy. At least three independent transformed strains were characterized for each construct.

Preparative and analytical techniques – Cells grown to a density of $4.10^6.ml^{-1}$ were broken in a "bead-beater" (Biospec-Products) according to the manufacturer's instructions. The membrane fraction was collected by centrifugation and resuspended in 10 mM Tricine, pH 8, at a chlorophyll concentration of 3 $g.l^{-1}$. For SDS-PAGE, membrane proteins were resuspended in 100 mM dithiothreitol and 100 mM Na_2CO_3 and solubilized by 2% SDS at 100 °C for 1 min. Polypeptides were separated on a 12-18% polyacrylamide gel containing 8 M urea (36). Immunoblotting was performed as described in ref. 3. The antiserum against PetL (7) was a kind gift of J.-D. Rochaix (Université de Genève). For the present work, antisera were prepared (Neosystem, Strasbourg, France) against peptides covering three regions of the predicted sequence of *C. reinhardtii* PetN precursor, namely PAAQAAQEVAMLAEG*, IVQIGWAATCVMFS* and *FSLSLVVWGRSGL (*cf.* Fig. 8; the asterisk indicates the site of coupling to the carrier protein). The only antiserum that yielded a positive reaction on

immunoblots was that raised against the C-terminal peptide, coupled to ovalbumin via its N-terminus. Other antipeptide antisera have been described in ref. 3. Cytochrome b_6f purification and electron transfer activity measurements were performed as described in ref. 3.

Optical and fluorescence measurement – Fluorescence measurements were performed at room temperature on a home built fluorimeter : samples were excited using a light source at 590 nm, and the fluorescence response was detected in the far-red region of the spectrum.

Absorbance measurements were performed at room temperature with a home built spectrophotometer described in refs. (37,38). Cells were re-suspended in the presence of 10 % Ficoll to avoid sedimentation. The slow phase of the electrochromic signal ("phase *b*" according to ref. 39), which is associated with electron transfer through the cytochrome b_6 hemes, was measured at 515 nm, where a linear response is obtained with respect to the transmembrane potential (40). Deconvolution of phase *b* from the membrane potential decay and calculation of cytochrome *f* redox changes were performed as described in ref. 41.

Protein phosphorylation assays – Cells were re-suspended in a phosphate-depleted medium containing 1 μCi ml^{-1} ^{33}Pi. They were treated as described in ref. 32. Polypeptides were separated by denaturing SDS-PAGE as described above. Autoradiography was performed as described in ref. 23.

Mass spectrometry – WT b_6f complex was purified and its subunits separated by SDS-PAGE and transferred onto nitrocellulose sheets (Millipore, Bedford, MA) according to ref. 3. Samples were localized on parallel lanes by combining immunoblotting with specific antibodies and staining with Ponceau red. The spots of interest were excised and fixed to a stainless steel target using double-sided tape. After several tests with different matrices, α-cyano-hydroxycinnamic acid acid (HCCA ; Sigma Chemical, Saint Louis, MO) was selected as the matrix of choice. Blot pieces were soaked into isopropanol and covered with a drop of the supernatant of a saturated solution of HCCA in acetone. After drying samples were washed

with acetonitrile. Extraction of chlorophyll by acetone prior to mass spectrometry resulted in the loss of part of the low-M_r peptides, the proportion of the smaller species (peaks around 3.5 kDa) diminishing considerably as compared with heavier ones (peaks around 4 kDa ; not shown). All analyzes therefore were performed without chlorophyll extraction. MALDI-TOF measurements were carried out on a STR Voyager mass spectrometer (Applied Biosystems, Framingham, CA) equipped with a nitrogen laser (237 nm, 20 Hz). Spectra were acquired in the linear positive mode (accelerating voltage 20 kV, grid voltage 95%), with a delayed extraction time of 300 ns. They were calibrated using a mixture of adrenocorticotropic hormone (residues 7-38 ; m/z = 3660.19 Da) and bovine insulin (m/z = 2867.80 Da and 5734.59 Da), which was applied directly to blot pieces.

RESULTS

Construction of C. reinhardtii *mutants expressing chimeric proteins* – Two chimeric proteins were constructed, both of them comprised of a full-length suIV fused, at its C-terminus, to the N-terminus of PetL (Fig. 1). They differed with respect to which of two AUG codons was considered as the initiation codon for PetL synthesis. As a result, the last transmembrane helix of suIV was connected to the single putative transmembrane helix of PetL by either a short or a long intervening loop (~20 and ~30 residues, respectively). The corresponding plasmids were named p*DL*S and p*DL*L. The chloroplast genome of the non-phototrophic Δ*petD* strain, which lacks the gene encoding suIV (29), was transformed by either plasmid. Both chimeric constructs yielded phototrophic clones. SDS-PAGE followed by immunoblotting with an anti-suIV antiserum showed that thylakoid membranes prepared from the transformed strains still lacked WT suIV. They accumulated instead a larger protein, whose size correlated with the expected size of the chimeras (Fig. 2). The same protein indeed also reacted with an

antiserum directed against PetL (not shown). The restoration of phototrophy therefore is not due to the presence of WT-like suIV, but to the fact that either of the two chimeric proteins can substitute for it.

In the absence of suIV, most other b_6f subunits are synthesized at WT rate, but rapidly degraded, and therefore do not accumulate (29,42). As expected given the phototrophy of the *DL*S and *DL*L strains, expression of either chimeric protein restored accumulation of the other b_6f subunits (Fig. 2), confirming that they assembled into a functional complex. A difference between the two strains however was consistently observed regarding WT PetL. This subunit, which was expressed in both cases along with the chimeric protein, accumulated to WT levels in the strain expressing the chimera with the short loop, *DL*S, but not in the presence of that with a long loop, *DL*L (Fig. 2). Since the b_6f complex is present and functional in *DL*L cells, it seemed likely that the chimeric protein could structurally and functionally substitute for *both* suIV and PetL.

Fig. 2

Chimeric PetL is able to stabilize the b_6f *complex in the absence of the endogenous subunit* – In order to test this hypothesis, the chloroplast genomes of strains *DL*L and *DL*S were transformed with plasmid p*ycf7*::*aadA*. This plasmid carries a *petL* coding sequence disrupted by the insertion of an *aadA* cassette, which confers resistance to spectinomycin (7). Transformed strains, named *DL*SΔ and *DL*LΔ depending on the recipient strain, were selected on spectinomycin-containing plates. Both types of strains were phototrophic and grew at a rate similar to that of the WT (not shown). Immunoblots of cells grown exponentially showed that they failed to accumulate either WT-like suIV or PetL (Fig. 2). On the other hand, the *DL*SΔ and *DL*LΔ strains accumulated the *DL*S or *DL*L chimeras, respectively, to levels similar to those observed for suIV in the WT strain (Fig. 2). The same held true for the other

b_6f subunits, indicating that in both cases the whole complex was properly assembled, with, apparently, a ~1:1 stoichiometry between the chimera and WT subunits (Fig. 2).

The stability of cytochrome b_6f is affected in Δ*petL* strains obtained by transformation of the WT with the *ycf7*::*aadA* plasmid : during exponential growth, the complex accumulates, although to somewhat reduced levels ; when cells enter the stationary phase, however, it disappears from thylakoid membranes (7). This behavior suggests that the absence of PetL renders the b_6f complex more sensitive to proteolytic degradation. The accumulation followed by disappearance of the b_6f complex in Δ*petL* mutants is reflected in their fluorescence induction kinetics upon illumination with actinic light : during exponential growth phase, fluorescence transients do not reach the maximum fluorescence yield obtained by adding the PSII inhibitor DCMU, a consequence of the PQ pool being reoxidized by cytochrome b_6f (43) ; in the stationary growth phase, on the contrary, fluorescence transients rise to a level similar to that measured in the presence of DCMU, due to the near-absence of cytochrome b_6f (ref. 7, and Figs. 3A and 3B).

Fig. 3

All chimeric mutant strains, when growing exponentially, exhibited fluorescence induction kinetics similar to those of the WT strain (not shown). This phenotype is consistent with the biochemical data, which show accumulation of cytochrome b_6f. In aging *DL*L and *DL*S mutant strains, fluorescence induction kinetics again reflected WT-like electron transfer (Fig. 3C). Aging *DL*LΔ and *DL*SΔ strains, on the other hand, behaved differently one from another : in *DL*LΔ, fluorescence transients indicated WT-like electron transfer, while in *DL*SΔ they betrayed a very slow rate of reoxidation of the plastoquinone pool (Fig. 3D). This point was further studied by comparing the accumulation of the main subunits of the b_6f complex in mutant strains expressing or lacking the endogenous PetL subunit. During the exponential phase (2.10^6 cells per ml), all chimeric strains resembled the WT, the presence or absence of

WT PetL having little or no effect on the level of accumulation of the other b_6f subunits (Fig. 4A). In aging cells (9.10^6 cells per ml), on the other hand, accumulation of the complex tended to be somewhat lower in strain *DL*LΔ and, even more so, in strain *DL*SΔ than in either WT or the *DL*L and *DL*S mutant strains (Fig. 4B).

Fig. 4

Biochemical stability of cytochrome b_6f complexes incorporating the DL*L chimeric protein* – PetL-free cytochrome b_6f complexes containing WT suIV, as accumulated during the exponential phase by Δ*petL* mutant strains, are markedly unstable following solubilization : upon sucrose gradient fractionation, they monomerize and release the Rieske protein (7). Cytochrome b_6f complex from the chimeric mutant strain *DL*LΔ, on the other hand, was still dimeric and functional after solubilization and purification on sucrose gradient. Subunit distribution along the gradient was similar to that for the WT complex (not shown) : the Rieske protein, in particular, comigrated with the other subunits, which is a reliable criterion of the integrity of the complex and its dimeric state (2). Nonetheless, *DL*LΔ complexes are more fragile than WT ones, and purification to homogeneity proved problematical.

Table I

Mass spectrometry analysis of the 4-kDa subunits – A structural interpretation of the above results depends in part on whether the putative 11-residue N-terminal extension of PetL, which makes up the difference between long and short loops in the chimeras, is part of the mature WT PetL subunit or not. In order to directly probe this point, preparations of purified WT cytochrome b_6f complex were submitted to SDS-PAGE and the peptides present in the low-M_r region analyzed by mass spectrometry. The results are summarized in Table I and Fig. 5. Of the three small subunits previously identified in *C. reinhardtii* b_6f complex, two yielded identifiable peaks. PetM appeared under two forms, one free and one acetylated. The sequence of the mature subunit starts at the position determined by Edman degradation (3,5,6)

and runs to the end of the open reading frame of the *petM* gene (8). PetG, although its presence has been established both immunologically (3,5) and by Edman degradation (6), was undetectable. PetL yielded two identifiable peptides. The first one was observed at three different masses, namely as its H^+, Na^+ and K^+ adducts. It starts with the methionine residue corresponding to the first AUG codon but stops after 30 residues rather than the 43 expected. The second, observed as an H^+ adduct only, starts with residue 5 (numbering from the first methionine) and ends at residue 39. It thus appears to be clipped by four residues at both termini. It should be noted that, given that this analysis failed to identify a peptide, PetG, that is undoubtedly present in the purified complex, the fact that no PetL peptide starting with the second methionine residue was recovered cannot be taken as a definite proof that this putative initiation site is not used at all.

Fig. 5

Interestingly, MALDI-TOF spectra also revealed the presence in purified preparations of WT *C. reinhardtii* b_6f of a fourth small subunit, PetN (Fig. 5 and Table I). Up till now PetN had been identified in Tobacco only, with strong evidence that in this organism it is an essential subunit of the b_6f complex (10). The nuclear genome of *C. reinhardtii* does contain a gene related to *N. tabacum petN* (11). Antisera were raised against one C-terminal and two putative N-terminal peptides predicted by the sequence of *C. reinhardtii petN* (Fig. 6A, boxes). Immunoblots of purified WT b_6f gave a positive signal with the anti-C-terminus serum only (Fig. 6B). Analysis of WT and Δ*petD* thylakoid membranes using this serum showed that PetN is absent in cells that do not accumulate the b_6f complex (Fig. 6B).

Fig. 6

State Transitions are abolished in the chimeric mutants – The occurrence of State Transitions in the chimeric mutants was examined by measuring the fluorescence yield of intact algae in the presence of the PSII inhibitor DCMU (43). PSI, at room temperature, acts as a

strong fluorescence quencher (15). Fluorescence emission therefore is proportional to the size of the PSII antenna and inversely proportional to the yield of PSII photochemistry (44). In the presence of DCMU, fluorescence changes during the transition from State 1 to State 2 thus directly reflect the decrease in PSII antenna size. Transitions were elicited in total darkness (see *Experimental Procedures*), in order to be independent of the electron transfer properties of the strains. The *DL*LΔ and *DL*SΔ mutants were compared *i)* to the WT, used as a positive control, *ii)* to a strain lacking cytochrome b_6f, the Δ*petD* strain, which undergoes no State Transitions (22), as a negative control, and *iii)* to the Δ*petL* strain (7). The maximal fluorescence yield of the WT strain dropped by about 40% in State 2 as compared to State 1 (Fig. 7, panel *A*). This reflects the transfer of a major fraction of LHCII from PSII to PSI. The same effect was observed in the case of the Δ*petL* mutant (panel *B*), showing that the absence of WT PetL by itself does not block State Transitions. On the contrary, neither the b_6f-free Δ*petD* mutant (panel *E*) nor the *DL*SΔ or the *DL*LΔ ones (panels *C* and *D*) displayed any decreased of fluorescence yield under conditions promoting State 2. Actually, the fluorescence yield *increased* slightly under these conditions, a phenomenon previously observed in strains locked in State 1 when the PQ pool is fully reduced (33). Very similar results were obtained with the *DL*L and *DL*S strains, both of which express WT PetL along with the fusion protein (not shown).

Fig. 7

DL*L*Δ *and* DL*S*Δ *mutants fail to activate LHC-kinase under State 2 conditions* – Fluorescence measurements indicate that in the *DL*LΔ and *DL*SΔ mutants LHCII is not transferred from PSII to PSI under State 2 conditions. In order to assess whether locking in State 1 is due to the absence of LHCII kinase activation, we examined *in vivo* protein phosphorylation. Thylakoid membranes were purified from cells that had been pre-incubated for 90 min with $^{33}P_i$ and placed for 20 min under State 1 or State 2 conditions in a $^{33}P_i$-free medium (32). Fig. 8 shows

the labeling pattern of the thylakoid membrane polypeptides of the WT and of the *DL*LΔ, *DL*SΔ, Δ*petD* and Δ*petL* mutants in the 25-40 kDa region. In the WT, the phosphorylation of LHCII polypeptides, LHC-P13 and LHC-P17, increased in State 2 as compared to State 1, whereas the PSII phosphoprotein D2 showed an opposite behavior, as previously reported (32). Consistently with fluorescence measurements, a similar phosphorylation profile was observed in the Δ*petL* strain, while a significantly lower level of phosphorylation of LHC-P13 and LHC-P17 was observed in the *DL*LΔ *DL*SΔ and Δ*petD* mutants under conditions that promote State 2. This phosphorylation profile is typical of State 1 (32). In the WT and Δ*petL* strains, several minor phosphoproteins were detected in the 15-20 kDa region under State 2 conditions. Those included PetO, a protein that interacts with cytochrome b_6f (45). None of these polypeptides showed significant phosphorylation in the *DL*LΔ, *DL*SΔ and Δ*petD* mutants (Fig. 8).

Fig. 8

The cytochrome b_6f *complex of the* DL*L*Δ *and* DL*S*Δ *mutants exhibits* WT*-like plasto-quinol oxidase activity* – The fluorescence measurements presented in Fig. 3 indicate that the overall connection between PSII and PSI via the b_6f complex is functional in the chimeric mutant strains. A blockade of State Transition was therefore unexpected, all b_6f mutants affected in State Transitions isolated so far exhibiting impaired redox activity (reviewed in ref. 46). We therefore measured the rate of several reaction steps of the Q-cycle in order to check whether the inhibition of State Transitions might be associated with some functional deficiency not involving the rate-limiting reaction (which is the only one affecting the fluorescence measurements presented in Fig. 3).

The catalytic cycle of cytochrome b_6f comprises oxidation of PQH_2 at a lumenal (Q_o) site of the protein complex, and reduction of PQ at a stromal (Q_i) site. According to the "Q-cycle" hypothesis (47,48), PQH_2 oxidation results in injecting electrons into two distinct electron transfer chains, one comprising the Rieske protein and cytochrome *f,* the other involving the

two b_6 hemes. This process can be studied spectroscopically by measuring the redox changes of cytochrome *f* (49). In addition, since the oxidation of the b_6 hemes results in a transfer of charges across the membrane, electron flow through cytochrome b_6 generates a measurable increase of transmembrane potential in the ms time range (causing the slow phase, called "phase *b*", of the electrochromic signal ; see ref. 39).

Fig. 9

Fig. 9 shows the results of such measurements in the WT, and in the *DL*LΔ and *DL*SΔ strains. The slow phase of the electrochromic signal is shown in panels *A* to *C*. Amplitudes are normalized to that of the fast phase ("phase *a*"), which, when PSII activity is inhibited by the addition of DCMU and hydroxylamine, is driven solely by PSI and is therefore proportional to the number of positive charges injected into the plastocyanine pool (43). Under our experimental conditions, reduction of the PQ pool is assured at the expense of cell metabolism (50) and the availability of PQH_2 at the Q_o site does not limit the kinetics of cytochrome b_6f (41). Redox changes of cytochrome *f* are shown in panels *D* to *F,* where oxidation and reduction phases correspond to negative and positive absorption changes, respectively.

Fig. 9 clearly indicates that the electron transfer properties of the complex were not affected by the *DL*LΔ and *DL*SΔ mutations : the rates of the single reactions ($t_{½} \approx$ 5-6 ms) were comparable to those observed in the WT (41). In green algae incubated in the dark, an electrochemical proton gradient builds up (51), which selectively slows down the reactions occurring at the Q_o site (38,51). Such a gradient was also observed in the two mutants, as indicated by the effects of the protonophore FCCP, the addition of which accelerated phase *b* (Fig. 9, *A* to *C*, circles) and the reduction of cytochrome *f* (Fig. 9, *D* to *F*, circles) in much the same manner as observed in the WT ($t_{½} \approx$ 2 ms). We conclude, therefore, that the main electron and proton transfer steps of the b_6f catalytic cycle are not affected in the *DL*LΔ and the *DL*SΔ mutants.

DISCUSSION

Ability of suIV-PetL chimeras to substitute structurally and functionally for the two subunits – In all mutant strains the chimera obtained by fusing suIV and PetL was expressed at a level comparable to that of suIV in WT strains. Immunoblots showed no trace of any proteolytic cleavage that could have regenerated WT-like subunits. In strains lacking suIV but retaining endogenous PetL, expression of any of the two chimeras restored phototrophy, accumulation of the b_6f subunits, and fluorescence transients and electron transfer rates characteristic of a native-like complex. Either of the two constructs therefore is able to structurally and functionally substitute for suIV, despite the presence of an unnatural C-terminal extension. The intensity of the bands containing the chimeric proteins is consistent with a ~1:1 stoichiometry of the chimera with respect to the other large subunits, suggesting that any excess fusion protein is degraded, in the same manner as non-assembled WT suIV is degraded in WT cells. There is little doubt that the suIV-like moiety of the chimeric proteins must fold and assemble correctly, and that it functionally replaces the missing suIV within the complex.

What then is the fate of the PetL-like moiety of the chimeras ? Our data indicate that this is a function of *i)* the length of the intervening loop and *ii)* the presence or absence of the WT PetL subunit. In the *DL*S strains, which contain the short-loop construct and express WT PetL, the latter accumulates to WT-like levels. It is, therefore, not accessible to proteolysis, as is the case with non-assembled PetL, and must be incorporated stoichiometrically into the modified complexes. Immunoblots indicate that the PetL-like extension of the chimera is not proteolytically trimmed. The *DL*S complexes therefore must comprise two copies of the PetL sequence, one free and one fused to suIV. The latter is likely to form an extra transmembrane helix. The fact that it interferes neither with the assembly nor with the functioning of the complex is compatible with the outlying position of the third helix of suIV that is suggested by

electron microscopy data (13 ; see below). It is an interesting observation that, even though it cannot occupy its proper position in the complex, this extra PetL-like sequence segment is not degraded, while free, non-assembled PetL is (7). Among several possible interpretations, a simple one would be that degradation of free WT PetL starts at the N-terminus (*i.e.*, as shown below, from the lumen).

In constructs with a long loop, on the contrary, there is every evidence that the PetL-like moiety can, and does, displace and substitute for the endogenous peptide: *i)* in strains that co-express WT PetL along with the long-loop chimera (*DL*L), PetL accumulates to very low levels as compared to that in WT cells or in cells harboring the short-loop construct ; the most straightforward interpretation of this phenomenon is that the C-terminal moiety of the long-loop chimera occupies the binding site of PetL, which, not being able to assemble, becomes proteolytically degraded ; *ii)* in strains that express the long-loop construct but no WT PetL (*DL*LΔ), a functional complex is nevertheless assembled ; it is much more stable than PetL-free complexes both *in vivo* (persistence in aging cells) and *in vivo* (resistance to detergent). Altogether, these observations strongly suggest that the PetL-like moiety of the long-loop construct is able to bind to the site normally occupied by PetL and, to a large extent even if not absolutely with the same efficacy, to exert its stabilizing effect on the complex. Biochemical and spectroscopic data offer evidence that the short-loop construct also confers functionality to PetL-free complexes ; the stability of the *DL*SΔ complexes in aging cells however appears marginal. The affinity of the PetL-like moiety of the short-loop chimera for the binding site of PetL indeed must be lower than that of the long-loop one, since, at variance with the latter, it is unable to efficiently compete with endogenous PetL for its binding site and, thereby, to provoke its degradation.

Implications for the transmembrane topology of PetL – The ability of the PetL-like moiety of the long-loop chimera to occupy the binding site of PetL and to functionally substi

tute for it is a strong indication that this region of the chimera must adopt the same transmembrane topology as PetL does in WT b_6f. Because the suIV-like moiety of the construct substitutes for suIV, it also must adopt the same topology as the parent subunit, which places the fusion point in the lumen (1,52). This result is consistent with the PetL-like moiety of the chimera, and, therefore, WT PetL itself, lying with its N-terminal end in the lumen (7). Can the opposite orientation however be totally ruled out ? There are two conceivable types of events that could permit the long-loop chimera to generate functional b_6f complexes even if WT PetL lies with its N-terminus in the stroma. Both assume that the PetL-like moiety imposes this topology to the corresponding region of the chimera. Such a phenomenon has been observed in polytopic proteins whose transmembrane topology had been genetically tampered with, such as the MalF subunit of the maltose transporter (53) or lactose permease (54 ; for a discussion, see ref. 55). The first mechanism assumes the stoichiometry of the chimera to the other b_6f subunits to remain 1:1, while the second one requires it to be 2:1.

Case 1. A fusion protein present as a single copy per b_6f monomer would have to insert with its N-terminus in the stroma, to fit the natural topology of suIV, and its C-terminus in the lumen, to suit the postulated orientation of PetL. It would not, therefore, adopt the expected 4-helix topology. This can occur in two ways: either *(i)* one of the helices in the suIV-like region does not insert, or *(ii)* the loop forms an additional transmembrane helix. Hypothesis *i* seems very improbable : *a)* the right positioning of the first two transmembrane helices of suIV is a *sine qua non* condition for the lumenal loop that links them, which forms part of the Q_o site, to adopt a correct conformation (23) ; *b)* mutations in the seventh helix of cytochrome *b*, which is the homologue of the third helix of suIV, affect the assembly of the mitochondrial cytochrome bc_1 complex (56) ; and *c)* topological signals in the PetL-like moiety of the fusion protein would tend to direct its C-terminal end, not the N-terminal one, towards the stroma (7) ; given that the N-terminal moiety of the chimera is probably already

inserted by the time the C-terminal one is released from the ribosome (insertion of chloroplast-encoded subunits appears to be mainly cotranslational ; see *e.g.* refs. 57-58, and references therein), it is difficult to understand either why or how the PetL-like moiety of the chimera would force the upstream suIV-like one to insert or rearrange with an aberrant topology. Hypothesis *ii* also appears quite far-fetched, the hydrophilic character of the loop, and, in the case of the *DL*S construct, its short length, making it very improbable that it should have any tendency to form an additional transmembrane helix.

Case 2. A second mechanism to be considered is based on the fact that many integral proteins can tolerate the presence of supernumerary transmembrane helices without loss of function (reviewed in refs. 55,59-61), as is actually observed here in the case of the *DL*S strains. In b_6f complexes incorporating two *DL*L chimeras per monomer, one of the two chimeric molecules could feature four helices and have its two termini in the stroma (Fig. 1), substituting for suIV, while the other would either have a distorted topology, as hypothesized above, or adopt a fully inverted orientation, providing a functional PetL-like region. This kind of mechanism cannot be *a priori* ruled out (it may well account for erroneous topological conclusions drawn from fusion experiments carried out on cytochrome b_{559} (62)). It holds however very little appeal in the case of suIV-PetL chimeras : first, as discussed above, insertion of the fused PetL-like sequence with its N-terminal end in the stroma seems unlikely to occur ; second, the presence of two copies of the chimera per complex, although difficult to rule out, is not supported by any data (see below).

It seems safe, therefore, to conclude that the transmembrane orientation of WT PetL must be that originally postulated (7), namely that its N-terminus faces the lumen.

PetL length and location in the complex – The length of the intervening loop clearly has a strong effect on the ability of the PetL-like moiety of the chimeras to compete with the WT PetL subunit. Whether this can be taken as an indication that, in the three-dimensional

structure of cytochrome b_6f, PetL lies far away from the last transmembrane helix of suIV depends on which AUG codon is used as an initiation site for the translation of PetL. It was not known, at the onset of this work, whether *C. reinhardtii* PetL contains or not the sequence segment predicted by the gene sequence upstream of the initiation site used in most other photosynthetic organisms (7). In order to ensure that at least one of the constructs would contain the complete sequence of WT PetL, the extension of the loop was therefore given the sequence of this N-terminal region. In view of the different properties exhibited by the long-loop and short-loop strains, the length of mature WT PetL was examined using mass spectrometry. While the two PetL-derived peptides detected had clipped extremities, the first initiation codon clearly had been used for their synthesis. The higher efficiency of long-loop constructs at competing with WT PetL and stabilizing PetL-free complexes then does not necessarily reflect spatial constraints : it may also be due to the N-terminal extension of PetL being functionally important. The functionality of the b_6f complex in the short loop *DL*SΔ strains and its marginal but improved stability *in vivo* as compared to Δ*petL* complexes indicate, on the other hand, that the extension is at least partially dispensable.

While there is no doubt that the chimeras can structurally and functionally substitute for both suIV and PetL, a structural interpretation of this phenomenon again depends on the number of chimeras per monomer. The simplest and most likely hypothesis is that a single chimera molecule occupies simultaneously both the suIV and the PetL sites. An alternative is that two distinct chimeras with the same transmembrane topology be involved, one providing its suIV moiety and the other the PetL one, which would leave the distance between the two sites undetermined. One may entertain doubts at the idea of the b_6f dimer accommodating eight redundant transmembrane helices without its functionality being compromised. Such a model however is difficult to rigorously rule out. Immunoblots give no indication that the stoichiometry of the chimera to the other b_6f subunits is 2:1 rather than than 1:1 ; however,

the ECL reaction used in the present study is far from being a quantitative assay. It could also be argued that proteolytic removal of unassembled suIV is so efficient that it is unlikely that chimera molecules with only the PetL moiety inserted into the complex would be totally spared and would not generate any fragments, which would have been detected in immunoblots. The argument holds some appeal… but it is weakened by the fact that, in *DL*S strains, the redundant PetL-like extension of the chimera, which is undoubtedly present, is *not* degraded.

Inhibition of State Transitions – The fusion of suIV and PetL inhibits State Transitions without affecting the electron transfer efficiency of the complex. This phenotype is novel, impairment of State Transitions being associated with the loss of PQH_2 oxidizing activity in all b_6f mutants hitherto studied (22,23).

The WT-like electron transfer properties of the chimeric mutants explains their being able to grow phototrophically. This phenotype is consistent with previous suggestions that PetL plays essentially a structural function, and is not involved in the catalytic cycle of the complex (7), and with the idea that the C-terminus of suIV is not directly involved in PQH_2 binding and oxidation. The latter is inferred from the comparison of subunit sequences in the b_6f and bc_1 complexes. The two cytochromes share the same catalytic cycle (reviewed in refs. 1,63,64). While very few changes are tolerated in substrate-binding sites, a larger variability affects other sequence regions (1). This is indeed the case of the site of gene fusion in our constructs : the C-terminus of suIV is free in the b_6f complex (1,63,64), while the seventh helix of cytochrome *b* (its homologue in the bc_1 complex) is connected to the eight and last transmembrane helix (65,66). Fusing PetL at this position actually re-creates a local topology identical to that in the corresponding region of cytochrome *b*.

Quinol binding to cytochrome b_6f is not modified in the mutants. The impairment of State Transitions thus suggests that they are affected in the transduction of the activating signal from the Q_o site to the kinase. This might take place at two levels : *(i)* the interaction of

the kinase with the b_6f complex and *(ii)* its diffusion away from the cytochrome, where LHCII phosphorylation takes place (reviewed in ref. 46). The absence of PetO phosphorylation in the mutants suggests that the fusion of suIV and PetL inhibits State Transitions at step *(i)*. At variance with LHCII, this b_6f-associated peptide indeed is phosphorylated upon PQH_2 binding to Q_o even when diffusion of the kinase is blocked reviewed in ref. 46). The lack of phosphorylation of PetO in the *DL*LΔ and *DL*SΔ mutants under State 2 conditions therefore suggests that the kinase is unable to interact with the b_6f complex of the mutants in a way leading to its activation.

A Mechanism for LHCII-kinase activation in thylakoid membranes – The phenotype of the chimeric mutants suggests that at least one of the two fused subunits is involved in the docking of the LHCII kinase to – or in its activation by – the WT b_6f complex. A direct involvement of PetL in kinase activation seems very unlikely : State Transitions occur in the Δ*petL* mutant, which lacks this subunit, and they are inhibited in the *DL*S strain, where a WT copy of PetL occupies its binding site. On the contrary, a role of suIV in both kinase binding and activation appears more readily conceivable. One unsolved issue in understanding LHCII-kinase activation is the mechanism by which PQH_2 binding to Q_o, on the luminal site of the membrane, activates an enzyme that operates in the stroma. One model involves conformational changes of the Rieske subunit (23,27,28), whose flexibility has been demonstrated in both the bc_1 (65,66) and b_6f (67,68) complexes. Recently, we have proposed (69) that the activating signal is transduced to the active site of the kinase via conformational changes occurring in the transmembrane region of the cytochrome b_6f. Recent electron microscopy data indeed suggest that such changes, which are peculiar of the b_6f complex, accompany the movements of the Rieske protein catalytic domain (13). They occur in two main regions of the protein : the monomer to monomer interface, *i.e.* close to the region where the redox cofactors are likely positioned, and a more outlying region of the dimer (13). Such movements might

promote the activation of the kinase, either by transducing directly the activating signal to its stromal catalytic domain, or by stabilizing an interaction between a kinase transmembrane domain and the b_6f complex : the existence of a transmembrane helix has been proposed at least in the case of the TAKs (26), which are likely involved in State Transitions (25), and the outermost region of conformational changes would be readily accessible to diffusing transmembrane proteins (*cf.* Fig. 10).

Fig. 10

In the frame of this model, the phenotypes of the chimeric mutants can be tentatively explained. This is illustrated in Fig. 10, which shows projection maps of the cytochrome b_6f complex calculated in the absence (grey) and presence (white) of stigmatellin (redrawn from ref. 13). The probable position of the three helices of suIV is indicated as I, II and III, as deduced from the comparison of the projection maps of the b_6f and bc_1 complexes calculated at the same resolution (68; see ref. 13 for a detailed discussion). It can be observed that a rearrangement seems to take place in the vicinity (*) of these three helices upon addition of a ligand of the Q_o site, stigmatellin. In particular, a new density appears close to helix III, which carries the C-terminus of suIV. The absence of State Transitions in the suIV-PetL chimeras might be due to the linker peptide interfering sterically with movements occurring in this region, and thereby preventing, directly or indirectly, either the docking of the kinase or its activation. This effect would be independent of the presence and position of PetL subunit and of the length of the linker peptide, as observed in the present work. A prediction of this model is that similar effects could be expected upon fusion to the C-terminus of suIV of any other peptide likely to form a transmembrane helix - possibly even of a soluble peptide.

PetN : a fourth small subunit of the C. reinhardtii b_6f *complex* – Mass spectrometry experiments performed in the course of this work revealed the presence, in preparations of WT *C. reinhardtii* b_6f complex, of a fourth small subunit, PetN, homologous to that previously

identified in *N. tabacum* (10). A serum raised against a peptide featuring the predicted C-terminal sequence of *C. reinhardtii* PetN (11) confirmed the presence of PetN in purified b_6f preparations and in thylakoid membranes from WT cells. It also demonstrated its absence in cells that do not accumulate the complex. PetN therefore is a *bona fide* subunit of *C. reinhardtii* cytochrome b_6f, inasmuch as it is present in the purified complex and it does not accumulate in its absence.

Genes homologous to Tobacco *petN* have been identified in cyanobacteria (70) and in all chloroplast genomes analyzed to date. The high degree of conservation of the open reading frame (Fig. 8A) suggests that it codes for a functionally important subunit. In Tobacco, indeed, knocking *petN* out yields plants that are photosynthetically incompetent (10). The predicted mature sequence of *C. reinhardtii petN* is very similar to that of its chloroplast-encoded homologues (Fig. 8A). It is, however, preceded by a transit peptide, which is exactly conserved in the closely related species *Volvox carteri*. If the transit peptide is cleaved by the thylakoid processing peptidase (*cf.* Fig. 8A), the N-terminus of mature PetN must lie in the thylakoid lumen and its C-terminus in the stroma. The position of the cleavage site however remains ambiguous. The peptide identified by MALDI-TOF features the predicted C-terminus of PetN, which is conserved in all photosynthetic organisms (Fig.8A). Its N-terminus, on the other hand, is not that expected from the consensus sequence for the thylakoid processing peptidase, which typically cleaves after an AXA motif (57,71). It seems likely that, as observed for PetL, the peptide identified by mass spectrometry does not correspond to the full-length mature protein. Upstream of the N-terminus observed by MALDI-TOF lie several AXA motifs. Two of them (underlined in Fig. 8A) are both close to the N-terminus of the MALDI-TOF fragment and consistent with the specificity of the peptidase. The absence of cross-reaction with an antiserum raised against the synthetic peptide PAAQAAQEVALMAEG (Fig.8A, dotted box) would be consistent with the mature protein starting only after the AQA triplet (Fig. 8A,

solid arrow). Further studies however will be required to directly establish the position of the cleavage site.

Conclusion – In summary, the experiments reported in the present work lead to the following conclusions : *i)* neither a free suIV C-terminus nor a free PetL N-terminus is required for the b_6f complex from *C. reinhardtii* to assemble and function ; this observation opens up interesting prospects for multiple tagging of the complex, as well as for the construction of other fusion proteins ; it is of interest also that an extra copy of PetL, tethered to the C-terminus of suIV, be protected from proteolytic degradation even though it is prevented by endogenous PetL to integrate into the complex ; *ii)* initiation of PetL synthesis starts at the first of the two AUG codons ; *iii)* PetL lies with its N-terminus in the lumen ; *iv)* in the three-dimensional structure of cytochrome b_6f, the N-terminus of PetL and the C-terminus of suIV must be within reach of each other ; *v)* cytochrome b_6f complexes incorporating suIV-PetL chimeras correctly assemble and transfer electrons efficiently ; nevertheless, *vi)* they are unable to carry out State Transitions ; it seems possible that the linker peptide interfere with movements occurring in the complex and thereby prevent the docking of the kinase or its activation ; finally, *vii)* the purified b_6f complex from *C. reinhardtii* contains an eight, hitherto unrecognized subunit, PetN.

ACKNOWLEDGMENTS

We are particularly grateful to J.-D. Rochaix et Y. Takahashi for the gift of anti-PetL antiserum and of the p*ycf7*::*aadA* plasmid, to Y. Pierre for his participation in the mass spectrometry experiments, to C. Breyton for discussion and for providing the data used for drawing Figure 10, and to Y. Choquet, D. Picot and F.-A. Wollman for useful discussions and/or comments on the manuscript.

REFERENCES

1. Berry, E. A., Guergova-Kuras, M., Huang, L.-s., and Crofts, A. R. (2000) *Annu. Rev. Biochem.* **69**, 1005-1075
2. Breyton, C., Tribet, C., Olive, J., Dubacq, J.-P., and Popot, J.-L. (1997) *J. Biol. Chem.* **272**, 21892-21900
3. Pierre, Y., Breyton, C., Kramer, D., and Popot, J.-L. (1995) *J. Biol. Chem.* **270**, 29342-29349
4. Haley, J., and Bogorad, L. (1989) *Proc. Natl. Acad. Sci. USA* **86**, 1534-1538
5. Pierre, Y., and Popot, J.-L. (1993) *C. R. Acad. Sci. (Paris), Ser. III* **316**, 1404-1409
6. Schmidt, C. L., and Malkin, R. (1993) *Photosynth. Res.* **38**, 73-81
7. Takahashi, Y., Rahire, M., Breyton, C., Popot, J.-L., Joliot, P., and Rochaix, J.-D. (1996) *EMBO J.* **15**, 3498-3506
8. de Vitry, C., Breyton, C., Pierre, Y., and Popot, J.-L. (1996) *J. Biol. Chem.* **271**, 10667-10671
9. Boronowsky, U., Wenk, S.-O., Schneider, D., Jäger, C., and Rögner, M. (2001) *Biochim. Biophys. Acta* **1506**, 55-66
10. Hager, M., Biehler, K., Illerhaus, J., Ruf, S., and Bock, R. (1999) *EMBO J.* **18**, 5834-5842
11. Asamizu, E., Nakamura, Y., Sato, S., Fukuzawa, H., and Tabata, S. (1999) *DNA Res.* **6**, 369-373
12. Berthold, D. A., Schmidt, C. L., and Malkin, R. (1995) in *Photosynthesis : from light to biosphere. Proceedings of the Xth International Congress on Photosynthesis*

(Mathis, P., ed) Vol. II, pp. 571-574, V vols., Kluwer Academic Publishers, Dordrecht, Montpellier

13. Breyton, C. (2000) *Biochim. Biophys. Acta* **1459**, 467-474
14. Pierre, Y., Breyton, C., Lemoine, Y., Robert, B., Vernotte, C., and Popot, J.-L. (1997) *J. Biol. Chem.* **272**, 21901-21908
15. Bonaventura, C., and Myers, J. (1969) *Biochim. Biophys. Acta* **189**, 366-383
16. Allen, J. F. (1992) *Biochim Biophys.Acta* **1098**, 275-335
17. Bennett, J. (1991) *Annu. Rev. Plant Physiol.* **42**, 281-311
18. Allen, J. F., Bennett, J., Steinback, K. E., and Arntzen, C. J. (1981) *Nature* **291**, 25-29
19. Elich, T. D., Endelman, M., and Matoo, A. K. (1997) *FEBS Lett.* **4111**, 236-238
20. Fulgosi, H., Vener, A. V., Altchmied, L., Hermann, R. G., and Andersson, B. (1998) *EMBO J.* **17**, 1577-1587
21. Horton, P., and Black, M. T. (1981) *Biochim. Biophys. Acta* **635**, 53-62
22. Wollman, F.-A., and Lemaire, C. (1988) In *Photocatalytic Production of Energy Rich Compounds* (Hall, D.O., & Grassi, G., ed.), pp.210-214, Elsevier Applied Science, London.
23. Zito, F., Finazzi, G., Delosme, R., Nitschke, W., Picot, D., and Wollman, F.-A. (1999) *EMBO J.* **18**, 2961-2969
24. Gal, A., Hauska, G., Herrmann, R., and Ohad, I. (1990) *J. Biol. Chem.* **265**, 19742-19749
25. Snyders, S., and Kohorn, B. D. (2001) *J. Biol. Chem.* **276**, 32169-32176
26. Snyders, S., and Kohorn, B. D. (1999) *J. Biol. Chem.* **274**, 9137-9140

27. Vener, A. V., Van Kan, P. J., Gal, A., Andersson, B., and Ohad, I. (1995) *J. Biol. Chem* **270**, 25225-25232

28. Vener, A. V., Van Kan, P. J., Rich, P. R., Ohad, I., and Andersson, B. (1997) *Proc. Natl. Acad. Sci. USA* **94**, 1585-1590

29. Kuras, R., and Wollman, F. A. (1994) *EMBO J.* **13**, 1019-1027

30. Harris, E. H. (1989) *The Chlamydomonas sourcebook. A comprehensive guide to biology and laboratory use.*, First Ed., Academic Press, San Diego

31. Sueoka, N. (1960) *Proc. Natl. Acad. USA* **46**, 83-91

32. Wollman, F.-A., and Delepelaire, P. (1984) *J. Cell Biol.* **98**, 1-7

33. Bulté, L., Gans, P., Rebéillé, F., and Wollman, F.-A. (1990) *Biochim. Biophys. Acta* **1020**, 72-80

34. Rochaix, J.-D. (1978) *J. Mol. Biol.* **126**, 597-617

35. Boynton, J. E., Gillham, N. W., Harris, E. H., Hosler, J. P., Johnson, A. M., Jones, A. R., Randoplh-Anderson, B. L., Robertson, D., Klein, T. M., Shark, K. B., and Sanford, J. C. (1988) *Science* **240**, 1534-1537

36. Piccioni, R. G., Bennoun, P., and Chua, N.-H. (1981) *Eur. J. Biochem.* **117**, 93-102

37. Joliot, P., Béal, D., and Frilley, B. (1980) *J. Chim. Phys.* **77**, 209-216

38. Joliot, P., and Joliot, A. (1994) *Proc. Natl. Acad. Sci. USA* **91**, 1034-1038

39. Joliot, P., and Delosme, R. (1974) *Biochim. Biophys. Avta* **357**, 267-284

40. Junge, W., and Witt, H. T. (1968) *Naturforschung* **23**, 244-254

41. Finazzi, G., Büschlen, S., de Vitry, C., Rappaport, F., Joliot, P., and Wollman, F.-A. (1997) *Biochemistry* **39**, 2867-2874

42. Choquet, Y., Stern, D. B., Wostrikoff, K., Kuras, R., Girard-Bascou, J., and Wollman, F.-A. (1998) *Proc. Natl Acad. Sci. USA* **95**, 4380-4385

43. Bennoun, P. (1970) *Biochim. Biophys. Acta* **216**, 357-363

44. Butler, W. L. (1978) *Ann. Rev. Plant Physiol.* **29**, 345-378

45. Hamel, P., Olive, J., Pierre, Y., Wollman, F.-A., and de Vitry, C. (2000) *J. Biol. Chem* **275**, 17072-17079

46. Wollman, F. A. (2001) *EMBO J.* **20**, 3623-3630

47. Mitchell, P. (1975) *FEBS Lett.* **57**, 137-139

48. Crofts, A. R., Meinhardt, S. W., Jones, K. R., and Snozzi, M. (1983) *Biochim. Biophys. Acta* **723**, 202-218

49. Joliot, P., Béal, D., and Delosme, R. (1998) *in The Molecular Biology of Chloroplast and Mitochondria in Chlamydomonas, eds Rochaix, J.-D., Goldschmidt M. and Mechant, S. (Kluwer Acad. Publ., The Netherlands)*, 433-439

50. Bennoun, P. (1982) *Proc. Natl. Acad. Sci. USA* **79**, 4352-4356

51. Finazzi, G., and Rappaport, F. (1998) *Biochemistry* **37**, 9999-10005

52. Crofts, A., Robinson, H., Andrews, K., Van Doren, S., and Berry, E. (1987) in *Cytochrome systems. Molecular Biology & Bioenergetics* (Papa, S., Chance, B., and Ernster, L., eds), pp. 617-631, Plenum Press, New York & London

53. McGovern, K., Ehrmann, M., and Beckwith, J. (1991) *EMBO J.* **10**, 2773-2782

54. Bibi, E., Verner, G., Chang, C.-Y., and Kaback, H. R. (1991) *Proc. Natl. Acad. Sci. USA* **88**, 7271-7275

55. Popot, J.-L., de Vitry, C., and Atteia, A. (1994) in *Membrane Protein Structure : Experimental Approaches* (White, S. H., ed), pp. 41-96, Oxford University Press, New York

56. Brasseur, G., Saribas, G. S., and Daldal, F. (1996) *Biochim. Biophys. Acta* **1275**, 61-69

57. Baymann, F., Zito, F., Kuras, R., Minai, L., Nitschke, W., and Wollman, F.-A. (1999) *J. Biol. Chem.* **274**, 22957-22967

58. Röhl, T., and van Wijk, K. J. (2001) *J. Biol. Chem.* **276**, 35465-35472

59. Popot, J.-L. (1993) *Curr. Opin. Struct. Biol.* **3**, 532-540

60. Popot, J.-L., and Saraste, M. (1995) *Curr. Opin. Biotech.* **6**, 394-402

61. Popot, J.-L., and Engelman, D. M. (2000) *Annu. Rev. Biochem.* **69**, 881-923

62. McNamara, V. P., Sutterwala, F. S., Pakrasi, H. B., and Whitmarsh, J. (1997) *Proc. Natl. Acad. Sci. USA* **94**, 14173-14178

63. Hope, A. B. (1993) *Biochim. Biophys. Acta* **1143**, 1-22

64. Cramer, W. A., Soriano, G. M., Ponomarev, M., Huang, D., Zhang, H., Martinez, S. E., and Smith, J. L. (1996) *Annu. Rev. Plant Physiol. Plant Mol. Biol.* **47**, 477-508

65. Iwata, S., Lee, J. W., Okada, K., Lee, J. K., Iwata, M., Rasmussen, B., Link, T., Ramaswamy, S., and Jap, B. K. (1998) *Science* **281**, 64-71

66. Zhang, Z., Huang, L., Shulmeister, V. M., Chi, Y.-I., Kim, K. K., Hung, L.-W., Crofts, A. R., Berry, E. A., and Kim, S.-H. (1998) *Nature* **392**, 677-684

67. Schoepp, B., Brugna, M., Riedel, A., Nieschke, W., and Kramer, D. M. (1999) *FEBS Lett.* **450**, 245-250

68. Breyton, C. (2000) *J. Biol. Chem.* **275**, 13195-131201

69. Finazzi, G., Zito, F., Barbagallo, R. P., and Wollman, F. A. (2000) *J. Biol. Chem* **276**, 9770-9774

70. Kaneko, T., Sato, S., Kotani, H., Tanaka, A., Asamizu, E., Nakamura, Y., Miyajima, N., Hirosawa, M., Sugiura, M., Sasamoto, S., Kimura, T., Hosouchi, T., Matsuno, A., Muraki, A., Nakazaki, N., Naruo, K., Okumura, S., Shimpo, S., Takeuchi, C., Wada, T., Watanabe, A., Yamada, M., Yasuda, M., and Tabata, S. (1996) *DNA Res.* **3**, 109-136

71. Zhou, J., Fernandez-Velasco, J. G., and Malkin, R. (1996) *J. Biol. Chem.* **271**, 6225-6232

Footnote

[1] The abbreviations and trivial names used are : cyt, cytochrome ; DCMU, 3-(3',4'-dichloroprenyl)-1-1-dimethylurea ; ECL, enhanced chemiluminescence ; FCCP, carbonylcyanide *p*-(trifluoromethoxy)phenylhydrazone ; HCCA, α-cyano-hydroxycinnamic acid ; HEPES, *N*-(2-hydroxyethyl)piperazine-*N'*-(2-ethanesulfonate) ; LHC, light harvesting complex ; MALDI, matrix-assisted laser desorption/ionization ; MS, mass spectrometry ; OOE3, oxygen evolving enhancer protein 3 ; PAGE, poly-acrylamide gel electrophoresis ; PCR, polymerase chain reaction ; PQ, plastoquinone ; PQH_2, plastoquinol ; PS, photosystem ; Q_o, plastoquinol binding site ; suIV, suIV ; TAKs, thylakoid-associated kinases ; TAP, Tris-acetate-phosphate ; TOF, time of flight ; WT, wild-type ; μE, microeinstein.

LEGENDS TO FIGURES

FIG. 1. **Sequence of *petL* and predicted topology of wild-type and chimera proteins**. *Panel A*, sequence of *petL* and predicted protein sequence (from ref. 7) ; *arrows* indicate the two possible initiation codons ; plasmids p*DL*L and p*DL*S start with the first and the second initiation codon, respectively ; *closed* and *open circles* mark the position of the two corresponding methionine residues, shown in the schemes of the next panels. *Panel B*, expected topology of the suIV-PetL chimeras and of PetL in the *DL*L (long loop) and *DL*S (short loop) mutant strains ; the suIV-like moiety of the chimeras is stippled, the PetL-like one solid grey ; circles indicate the position of the methionine residues marked in *Panel A*. *Panel C*, in the *DL*LΔ and *DL*SΔ mutant strains, the chimeras are the same, but the endogenous *petL* gene has been inactivated.

FIG 2. **Immunoblot analysis of cytochrome b_6f subunits in wild-type and mutant strains.** Immunoblot analysis of the accumulation of suIV, PetL, cytochrome *f* (Cyt. *f*) and the Rieske protein in WT, Δ*petL* and transformant strains. Thylakoid membrane (containing 20 μg of chlorophyll) were subjected to SDS-PAGE and blots probed with subunit-specific antisera against subunits IV and PetL (see *Experimental Procedures*). Sera were used at 1/10,000 dilution and detected using the ECL system (Amersham). The PSII OEE3 protein was used as an internal control.

FIG. 3. **Fluorescence induction curves of dark-adapted Δ*petL* and transformant cells.** *Panel A*, Δ*petL* strain in the exponential growth phase ; F_0 : initial fluorescence yield due to open PSII centers (oxidized primary quinone acceptor) ; F_{max} : maximal fluorescence yield due to closed PSII centers (reduced primary quinone acceptor) ; F_{stat} : stationary level of

fluorescence, representative of the steady state level of reduction of the primary quinone acceptor under continuous illumination. *Panel B*, Δ*petL* strain in the stationary growth phase : F_{max} and F_{stat} are similar, which reflects the blockade of photosynthetic electrons transfer. *Solid line* : control ; *dotted line* : DCMU 10μM (closed PSII centers). *Panels C* and *D*, stationary phase data for the four chimeric strains ; *dashed* and *solid lines* refer to strains harboring the *DL*S or the *DL*L chimera, respectively ; *dotted line*: DCMU 10 μM.

FIG. 4. **Accumulation of cytochrome b_6f subunits in thylakoid membranes from wild-type and mutant strains in exponential and stationary growth phases.** Experimental conditions were the same as in Fig. 2.

FIG. 5. **Mass spectrometry analysis of low M_r subunits from purified wild-type b_6f complex.** MALDI-TOF analysis following SDS-PAGE and electroblotting (see *Experimental Procedures*). The mass of each identified peak corresponds uniquely to that calculated for the indicated stretch from the predicted sequences of the four 4-kDa subunits. See TABLE I.

FIG. 6. **Sequence alignment and immunoblot analysis of PetN.** *Panel A*, alignment of the *petN*-derived amino acid sequences from *C. reinhardtii* and selected other photosynthetic organisms. The sequence of the peptide identified by MALDI-TOF is indicated in *bold*. *Panel B*, immunodetection of PetN in the 4-kDa region of SDS-PAGE blots of purified cytochrome b_6f (Cyt. b_6f) and of thylakoid membranes from wild-type (WT) and Δb_6f cells. The antiserum was raised against a synthetic peptide corresponding to the C-terminus of PetN (*Panel A*, solid box), used at 1/1,000 dilution and detected with the ECL system.

FIG. 7. **Consequences of the Δ*petL*, Δ*petD*, *DL*LΔ and *DL*SΔ mutations on State Transitions.** *A*, WT ; *B*, Δ*petL* ; *C*, *DL*SΔ ; *D*, *DL*LΔ ; *E*, Δ*petD*. Cells were harvested during exponential phase of growth and resuspended in minimal medium (32). *Continuous line* : State 1 promoting conditions (vigorous agitation in the dark in air) ; *dashed line* : State 2 promoting conditions (addition of 5 μM FCCP). All measurements were carried out in the presence of 10 μM DCMU.

FIG. 8. **Autoradiogram of ^{33}P radiolabeled antenna polypeptides in the 15-35 kDa region.** Cells were placed in State 1 or State 2 conditions as in Fig. 7. Other conditions as in Figure 7. (*) PetO protein.

FIG. 9. **Slow electrochromic phase (panels *A* to *C*) and time-resolved redox changes of cytochrome *f* (panels *D* to *F*) in WT (panels *A* and *D*), *DL*SΔ (panels B and E) and *DL*LΔ (panels *C* and *F*) strains.** Algae were illuminated with non saturating flashes (20% of saturation), given 6.6 s apart under anaerobic conditions. Measurements were performed in the absence (squares) and presence (circles) of 1 μM FCCP. Lines represent the best fit to data points using either single (panels *A* to *C*) or double (panels *D* to *F*) exponentials.

FIG. 10. **Comparison of the projection maps of cytochrome b_6f in the presence and absence of stigmatellin.** Projection maps obtained by cryo-electron microsopy at 10 Å resolution in the absence (grey) and presence (white) of stigmatellin. Probable positions of the three transmembrane helices of suIV are labeled I-III. Stigmatellin-induced conformational changes occurring close to suIV (*). Redrawn from ref. 13. See text.

TABLE I. Low M_r peptides identified by MALDI-TOF in purified preparations of wild-type cytochrome b_6f complex.

Subunit, residues, associated ion	Average mass	Sequence
PETL(1-30)+H^+	3467.24	**M**IFDFNYIHIF**M**LTITSYVGLLIGALVFTL
PETL(1-30)+Na^+	3489.24	
PETL(1-30)+K^+	3505.24	
PETN(13-45)+H^+	3483.07	AEGEPAIVQIGWAATCVMFSFSLSLVVWGRSGL
PETN(13-45)+Na^+	3505.07	
PETN(13-45)+K^+	3521.07	
PETL(5-39)+H^+	3917.82	FNYIHIF**M**LTITSYVGLLIGALVFTLGIYLGLLKV
PETM(1-39)+H^+	4035.82	GEAEFIAGTALTMVGMTLVGLAIGFVLLRVESLVEEGKI
PETM(1-39)Ac+H^+	4077.82	

A

p*DL*L p*DL*S

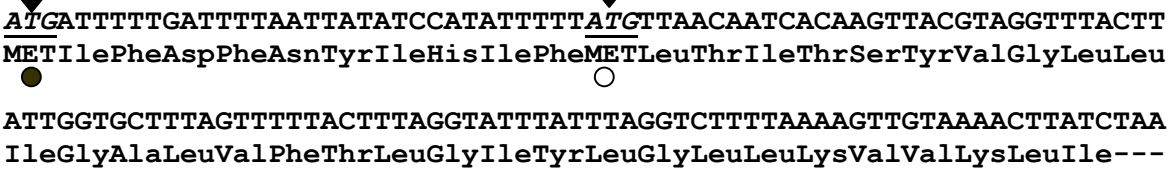

B *DLS*/*DL*L

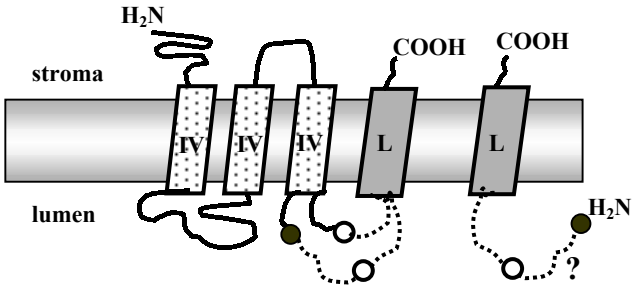

C *DLS*Δ/*DL*LΔ

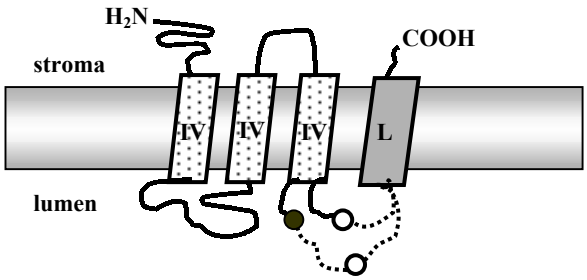

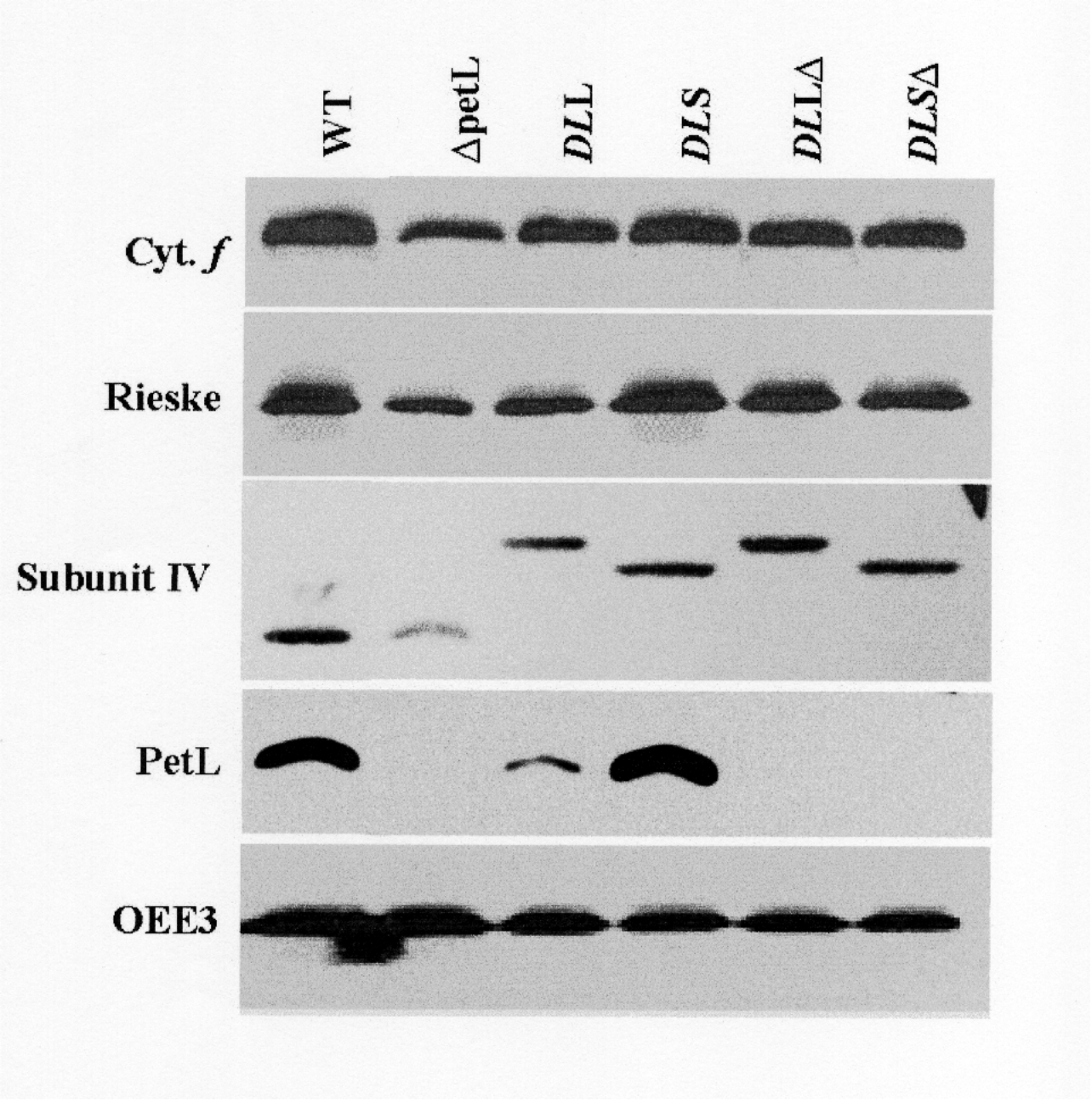
WT
ΔpetL
DLL
DLS
DLLΔ
DLSΔ
Cyt. f
Rieske
Subunit IV
PetL
OEE3

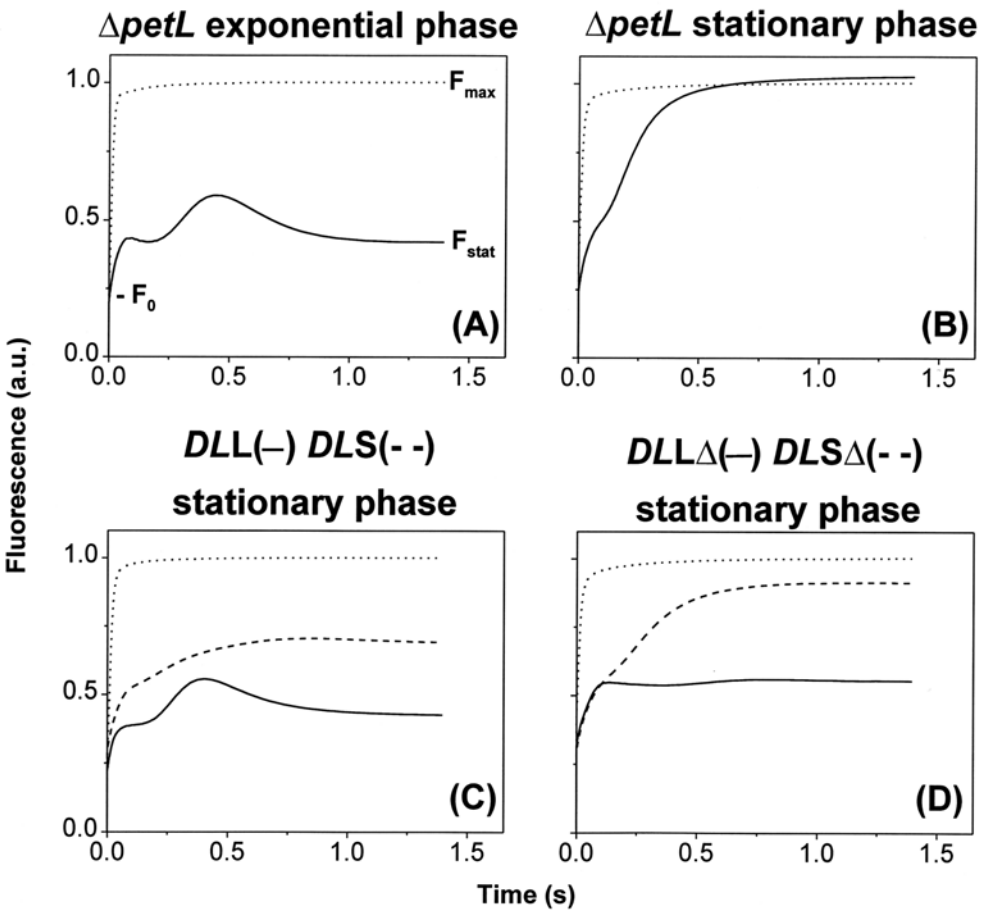
ΔpetL exponential phase
ΔpetL stationary phase
DLL(–) DLS(- -)
stationary phase
DLLΔ(–) DLSΔ(- -)
stationary phase
Fmax
Fstat
- F0
(A)
(B)
(C)
(D)
Fluorescence (a.u.)
Time (s)
0.0
0.5
1.0
1.5

A

B

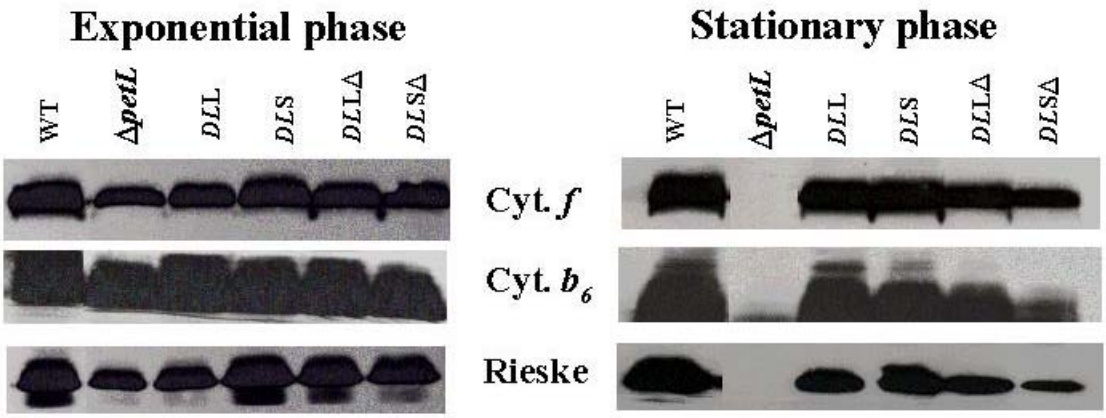
Exponential phase
Stationary phase
WT
ΔpetL
DLL
DLS
DLLΔ
DLSΔ
Cyt. f
Cyt. b6
Rieske

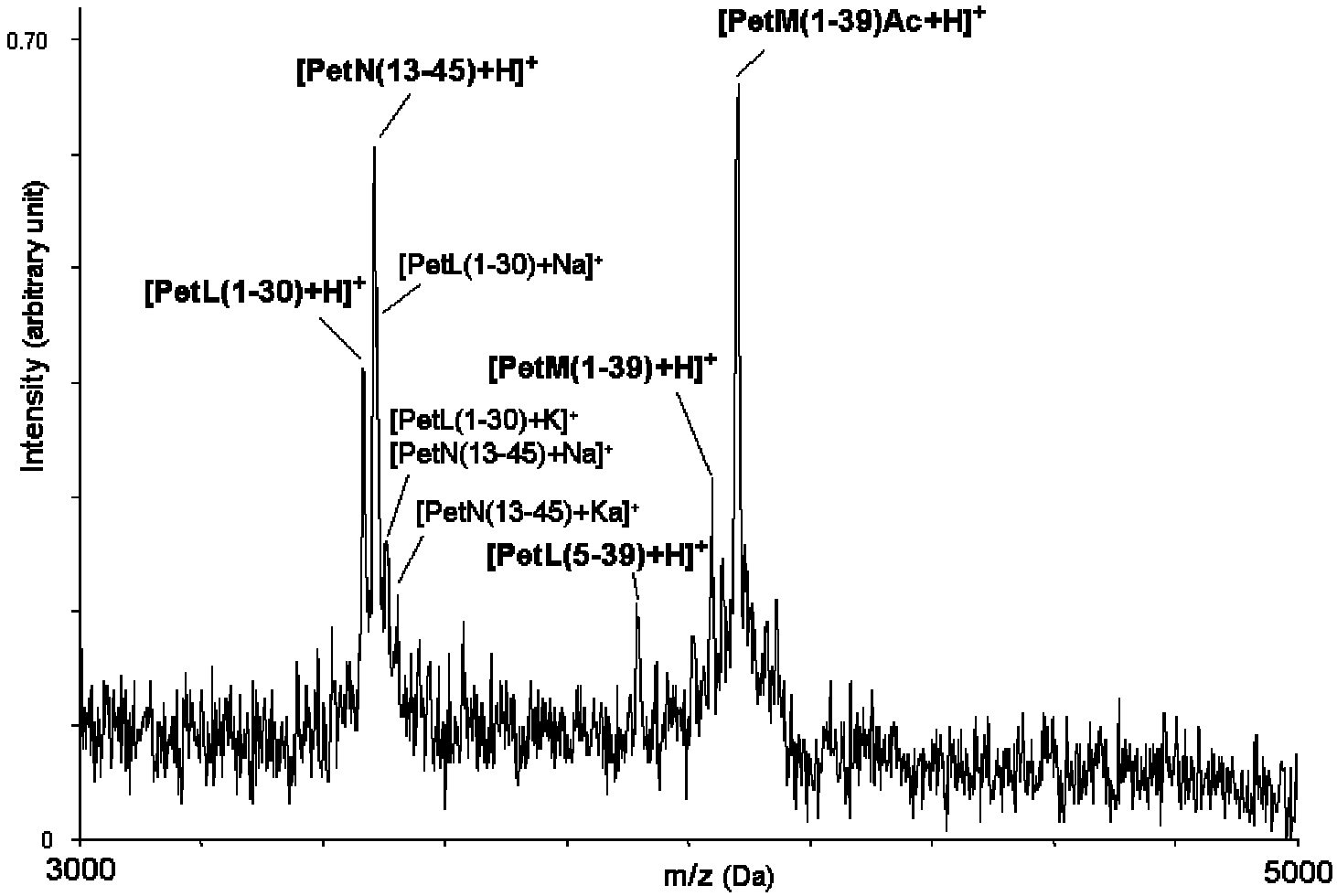
0.70
0
Intensity (arbitrary unit)
3000
m/z (Da)
5000
[PetM(1-39)Ac+H]+
[PetN(13-45)+H]+
[PetL(1-30)+Na]+
[PetL(1-30)+H]+
[PetM(1-39)+H]+
[PetL(1-30)+K]+
[PetN(13-45)+Na]+
[PetN(13-45)+Ka]+
[PetL(5-39)+H]+

A

PAIVQIGWAATCVMFSFSLSLVVWGRSGL	*C. reinhardtii* and *V. carteri*
MDIVSLAWAALMVVFTFSLSLVVWGRSGL	*N. tabacum*
MDIVGITWAALMVVFTFSLSLVVWGRSGL	*P. thunbergii*
MDIINIAWAALMVIFTFSLSLVVWGRSGL	*M. polymorpha*
MAILTLGWVSLLVVFTWSIAMVVWGRNGL	*A. variabilis*
MDILSLGWAALMAMFTFSIAMVVWGRNGF	*P. purpurea*
MDILTLGWVSVLVLFTWSISMVVWGRNGF	*Synechocystis sp. PCC680*

***C. reinhardtii* predicted *petN* precursor**

MQCVSRVAQRSAVSRPRVASRQAVKVQAVKAESKAAMAAVAAGASTLALALA

PAAQAAQEVAML**AEGEPAIVQIGWAATCVMFSFSLSLVVWGRS**

PP ? MS

B

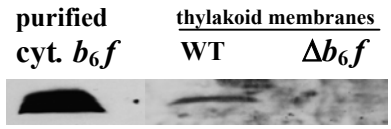

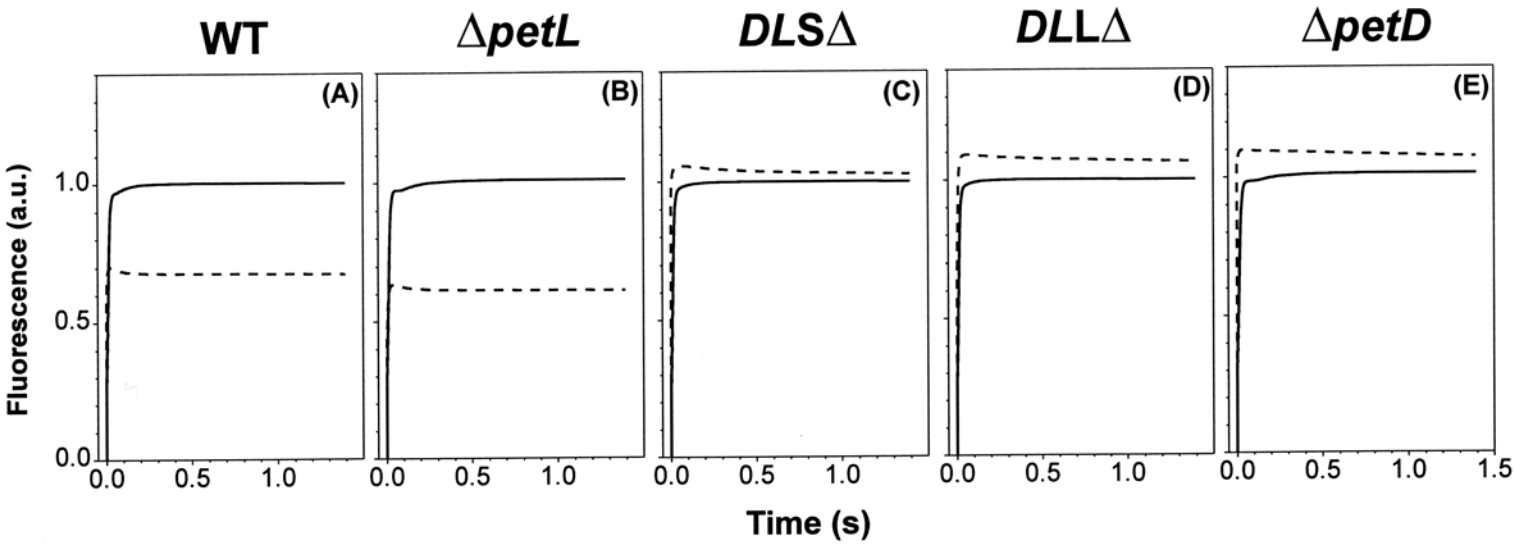
WT
ΔpetL
DLSΔ
DLLΔ
ΔpetD
(A)
(B)
(C)
(D)
(E)
Fluorescence (a.u.)
1.0
0.5
0.0
0.0
0.5
1.0
1.5
Time (s)

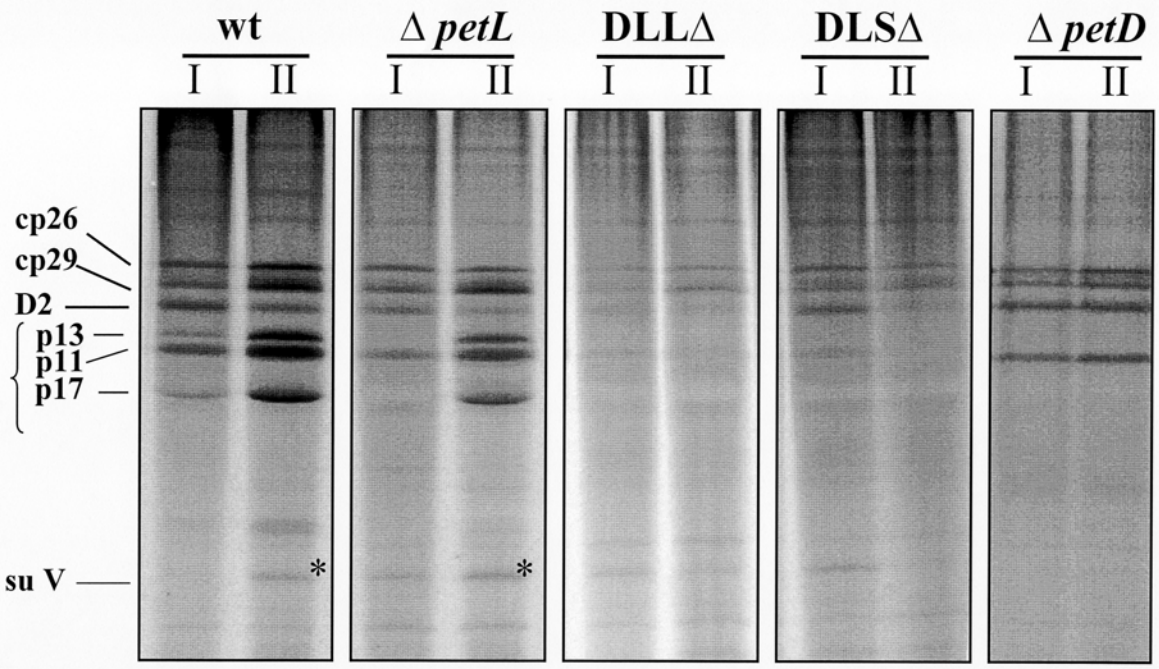
wt
Δ petL
DLLΔ
DLSΔ
Δ petD
I
II
cp26
cp29
D2
p13
p11
p17
su V
*
*

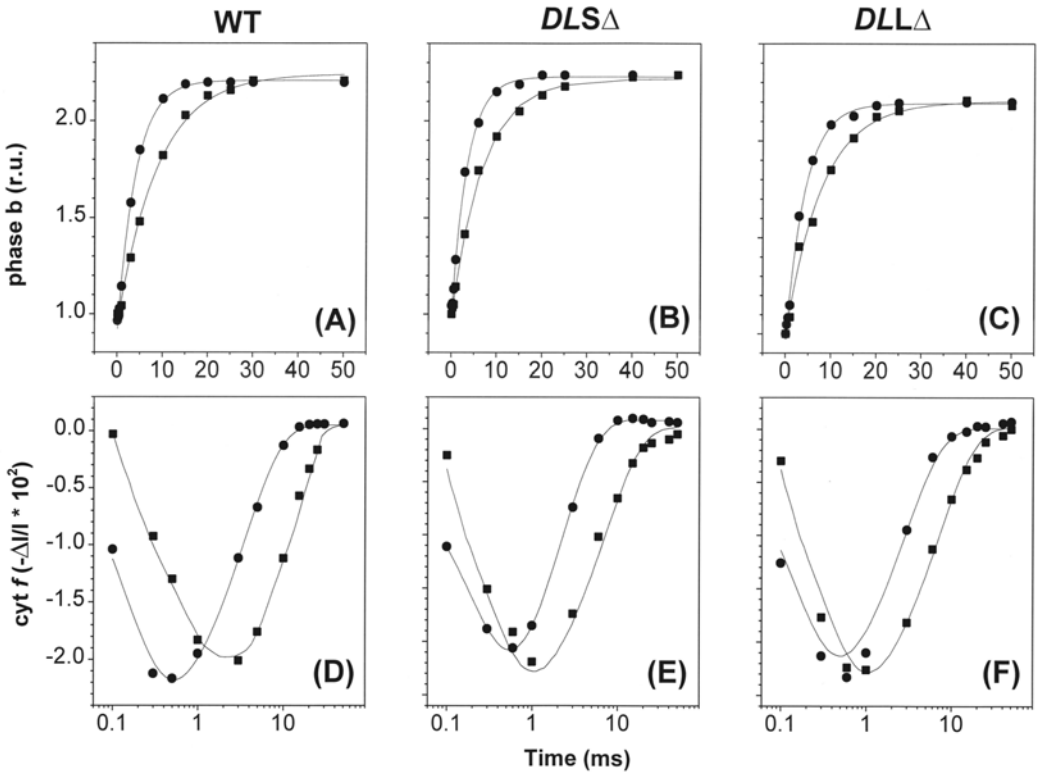
WT
DLSΔ
DLLΔ
phase b (r.u.)
2.0
1.5
1.0
(A)
(B)
(C)
0
10
20
30
40
50
cyt f (-ΔI/I * 10²)
0.0
-0.5
-1.0
-1.5
-2.0
(D)
(E)
(F)
0.1
1
10
Time (ms)

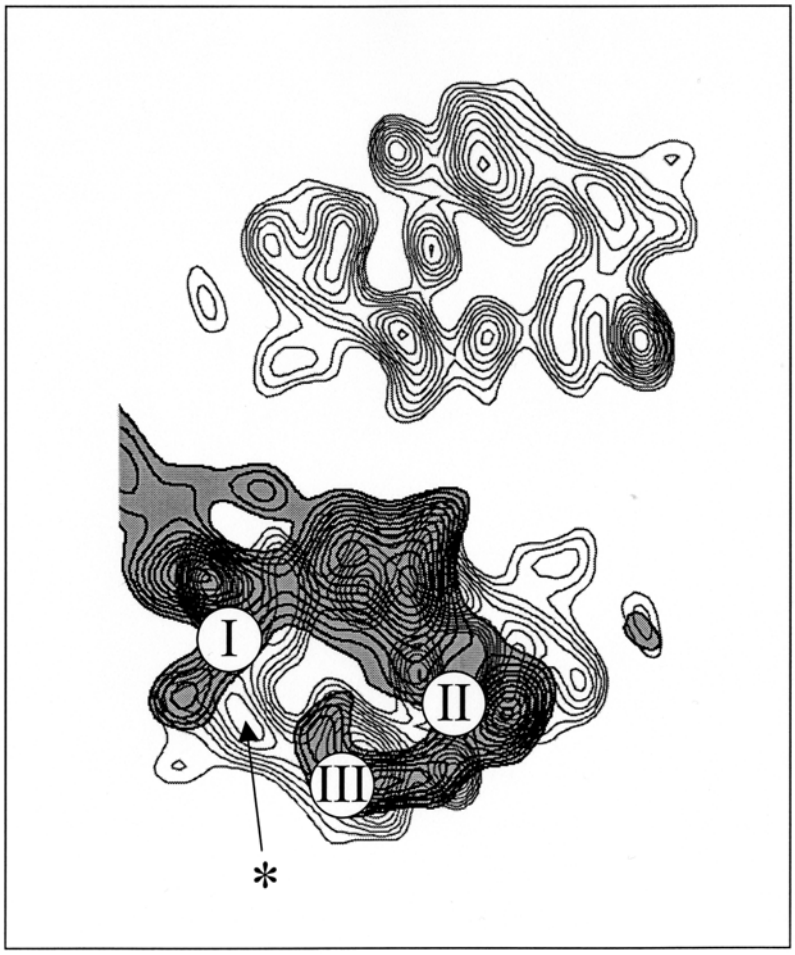
I
II
III
*